Electronic Supporting Information

Molecular Signature of Polyoxometalates in Electron Transport of Silicon-based Molecular Junctions

Maxime Laurans, Kevin Dalla Francesca, Florence Volatron, Guillaume Izzet, David Guerin, Dominique Vuillaume,* Stéphane Lenfant,* Anna Proust**

Content

Figure S10. Cyclic voltammogram of a $\mathbf{K^{Mo}_{Sn}}$-functionalized glassy carbon electrode in a 0.1M $TBAPF_6$ solution in acetonitrile at scan rate of $\nu = 100$ mV.s^{-1}.

3. XPS Characterization

Figure S11**.** P2p and O1s HR-XPS spectra of $\mathbf{K^{W}_{Sn}}$ modified n-Si(100) substrate

Figure S12. $Sn3d_{5/2}$, N1s, C1s and P2p HR-XPS spectra of a $\mathbf{K^{W}_{Mo}[N_2^+]}$ reference powder drop-casted on a Si/SiO_2 substrate.

Figure S13. $Sn3d_{5/2}$, N1s, C1s, P2p and O1s HR-XPS spectra of $\mathbf{K^{Mo}_{Sn}}$ modified n-Si(100) substrate.

Figure S14. Mo3d HR-XPS spectrum of (left) the $\mathbf{K^{Mo}_{Sn}[N_2^+]}$ powder reference and (right) the $\mathbf{K^{Mo}_{Sn}}$ modified n-Si(100) substrate.

4. Current histograms at -1V and 1V on K^{W}_{Sn} and K^{Mo}_{Sn} monolayers grafted on highly doped Si substrate

Figure. S15. Histograms of the measured current at +1V and -1V for the K^{W}_{Sn} and K^{Mo}_{Sn} samples.

5. I-V curves adjustment with the Simmon's equation

6. Histograms of effective mass obtained by Simmon's adjustments on K^{W}_{Sn} and K^{Mo}_{Sn} monolayers

Figure. S16. Reduced mass (m_r) histograms obtained by Simmon's adjustments on the different I-V curves, and adjusted by a Gaussian distribution for the K^{Mo}_{Sn} and K^{W}_{Sn} derivatized monolayers.

1. NMR and ESI-MS characterization of $TBA_4[PW_{11}O_{39}\{Sn(C_6H_4)C{\equiv}C(C_6H_4)N_3(C_2H_5)_2\}]$ $K^W_{Sn}[N_3Et_2]$ and $TBA_3[PW_{11}O_{39}\{Sn(C_6H_4)C{\equiv}C(C_6H_4)N_2\}]$ $K^W_{Sn}[N_2^+]$

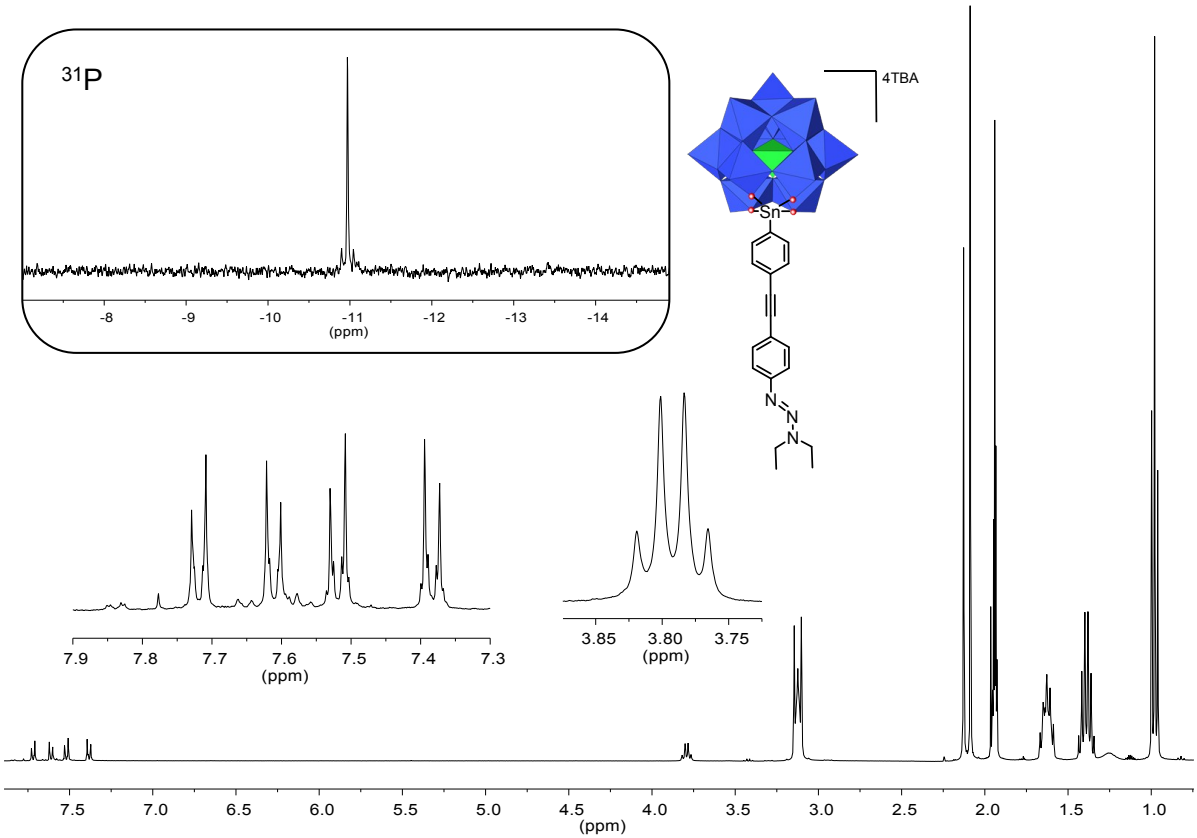

Figure S1. ^1H (400 MHz) and ^{31}P (121.5 MHz, framed inset) NMR spectra of $\mathbf{K^W_{Sn}[N_3Et_2]}$ in CD_3CN.

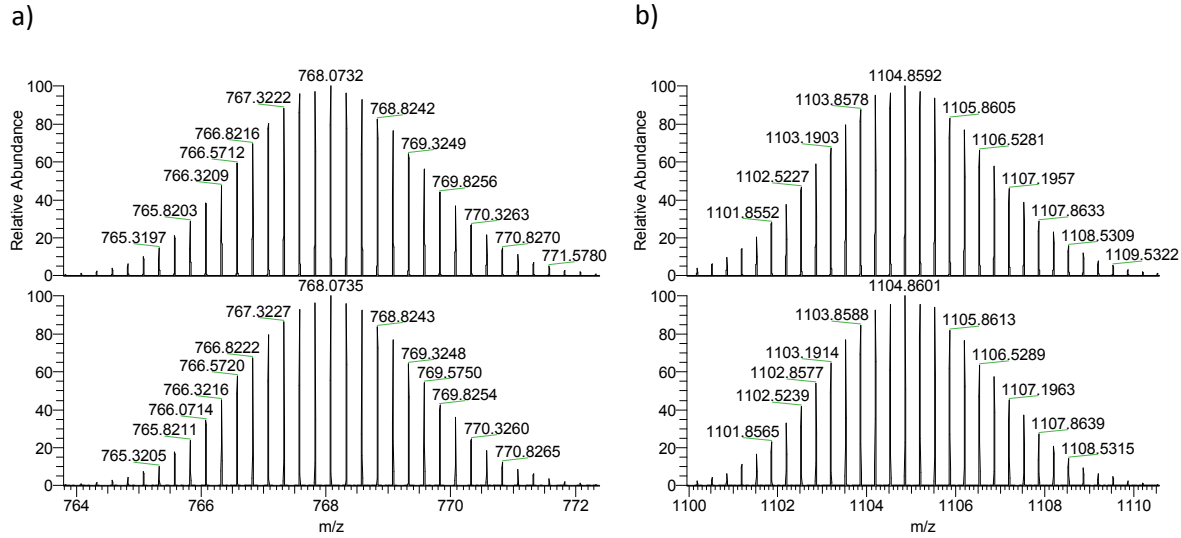

Figure S2. Comparison of experimental (lower trace) and calculated (upper trace) isotopic

peaks for the most abundant ions i.e. : a) $[POM]^{4-}$ calcd 768.07 found 768.07 ; b) $[POM+TBA]^{3-}$ calcd 1104.86 found 1104.86. POM = $[PW_{11}O_{39}\{Sn(C_6H_4)C{\equiv}C(C_6H_4)N_3(C_2H_5)_2\}]$

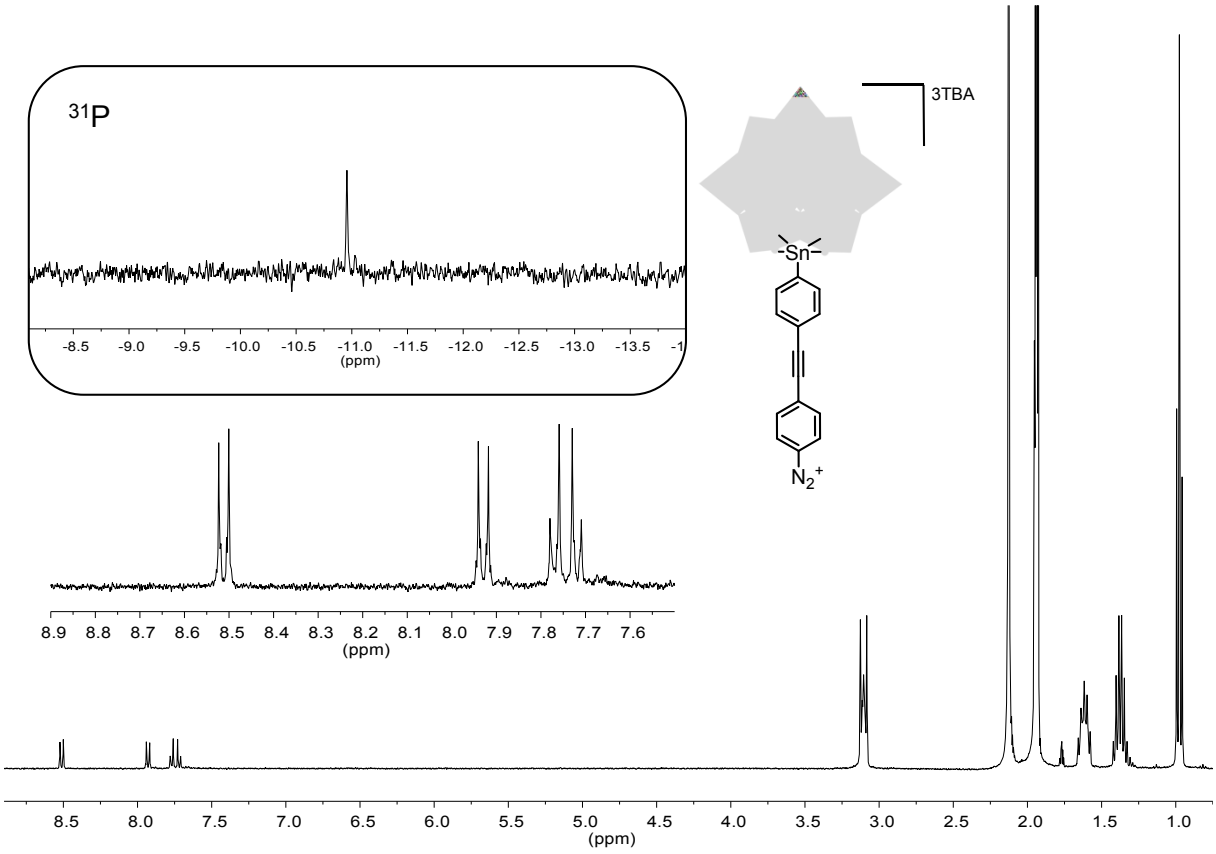

Figure S3. ^{1}H (400 MHz) and ^{31}P (121.5 MHz, framed inset) NMR spectra of $\mathbf{K^{W}_{Sn}[N_2^+]}$ in CD_3CN.

2. Cyclic voltammetry

Cyclic voltammetry

Electrochemical studies were performed on an Autolab PGSTAT 100 work station (Metrohm) using a standard 3-electrode setup filled with a 0.1 M solution of tetrabutylammonium hexafluorophosphate electrolyte in acetonitrile kept under argon. The electrochemical properties of the POMs in solution (1 mM) were investigated with a glassy carbon electrode (3 mm diameter) that was polished with 6 µm diamond paste, sonicated in ethanol for 5 min and dried with an argon flow. Alternatively the POM-modified silicon wafer itself was used as the working electrode. Platinum wire and saturated calomel electrode (SCE) equipped with a double junction were used as auxiliary and reference electrodes respectively. Grafting of $TBA_3[PM_{11}O_{39}\{Sn(C_6H_4)C{\equiv}C(C_6H_4)N_2\}]$ (**$K^{M}_{Sn}[N_2^+]$**) onto glassy carbon was achieved as previously described by cycling around the reduction wave of the diazonium function (between -0.2 and -0.8 V/SCE),[1,2] the modified electrode was then thoroughly rinsed and sonicated in DMF and acetonitrile before its characterization.

V/SCE	$E_{p,red}$	$E_{p,ox}$	$E_{1/2}$= ½($E_{p,red}$+$E_{p,ox}$)
$TBA_4[PW_{11}O_{39}\{SnC_6H_4I\}]$ (**K^{W}_{Sn}[I]**)			-0.97 -1.42 [3]
$TBA_4[PW_{11}O_{39}\{Sn(C_6H_4)C{\equiv}C(C_6H_4)N_3Et_2\}]$ (**$K^{W}_{Sn}[N_3Et_2]$**)	-1.07	-0.94	-1.00
K^{W}_{Sn}-modified glassy carbon electrode	-1.03	-1.00	-1.01
K^{W}_{Sn}-modified Si(100) electrode	-1.03	-0.93	-0.98
$TBA_4[PMo_{11}O_{39}\{SnC_6H_4I\}]$ (**K^{Mo}_{Sn}[I]**)			-0,50 -0,92 [4]
$TBA_4[PMo_{11}O_{39}\{Sn(C_6H_4)C{\equiv}C(C_6H_4)N_3Et_2\}]$ (**$K^{Mo}_{Sn}[N_3Et_2]$**)			-0.50
K^{Mo}_{Sn}-modified glassy carbon electrode			-0.55 [2] -0.52

Table S1. Mid-point redox potentials (versus SCE) from cyclic-voltammograms recorded at 100 mV s^{-1} for POM hybrids in solution or covalently immobilized onto the working electrode.

For reasons that we do not fully explained at the moment it was not possible to recover well defined waves from the **K^{Mo}_{Sn}**-POMs grafted onto silicon. This might arise from a too fast growing of an insulting SiO_2 layer, which is very difficult to avoid when working in solution or from the presence of traces of protons, introduced in the last step of the synthesis of **$K^{Mo}_{Sn}[N_2^+]$**. This is particularly acute for molybdates that are more sensitive to protonation than their corresponding tungstates. Deliberate addition of protons results first in a broadening of the electrochemical waves and it is only at high proton concentrations that well-resolved waves are recovered, usually at higher potentials. This has been discussed in a previous contribution related to the immobilization of **$K^{Mo}_{Sn}[N_2^+]$** onto glassy carbon electrode.[2] We have indeed observed that the shape of the electrochemical waves of the **K^{Mo}_{Sn}**-modified glassy carbon electrode was altered compared to the case of a **K^{W}_{Sn}**-modified glassy carbon electrode.[1,2]

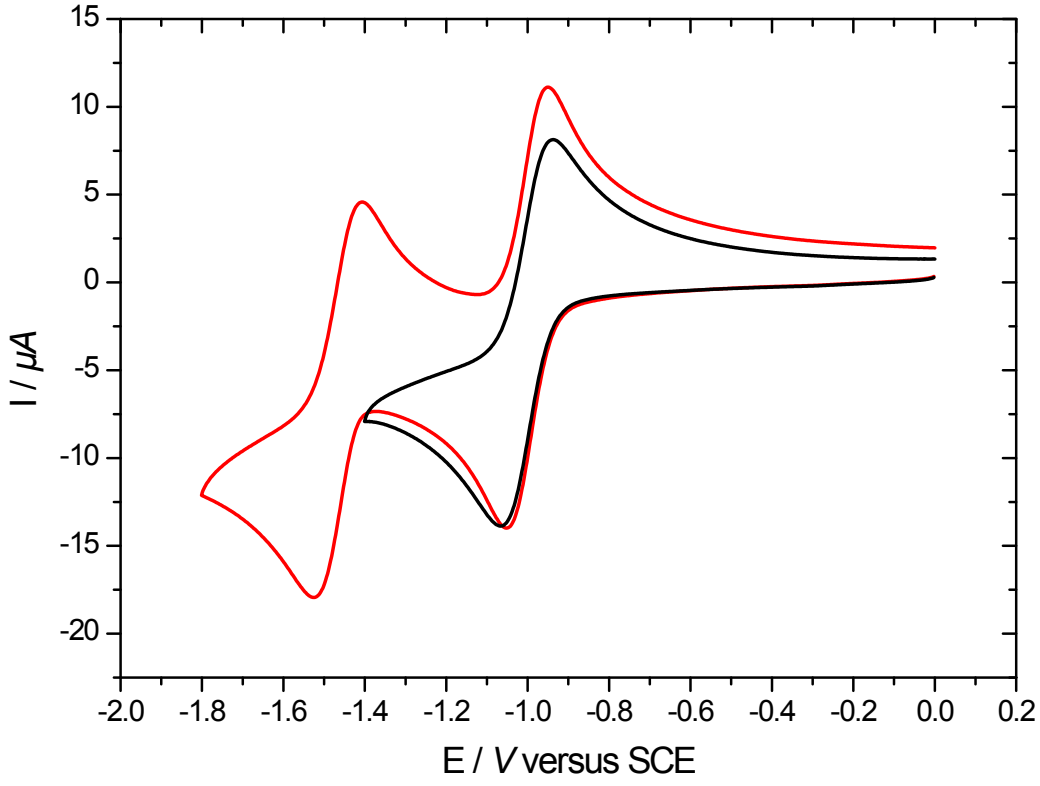

Figure S4. Cyclic voltammogram of $\mathbf{K^{W}_{Sn}[N_3Et_2]}$ (1mM) at a GC electrode in a 0.1M $TBAPF_6$ solution in acetonitrile at scan rate of $\nu = 100$ mV.s^{-1}. $E_{1/2}{}^{red1} = -1.00V_{/SCE}$

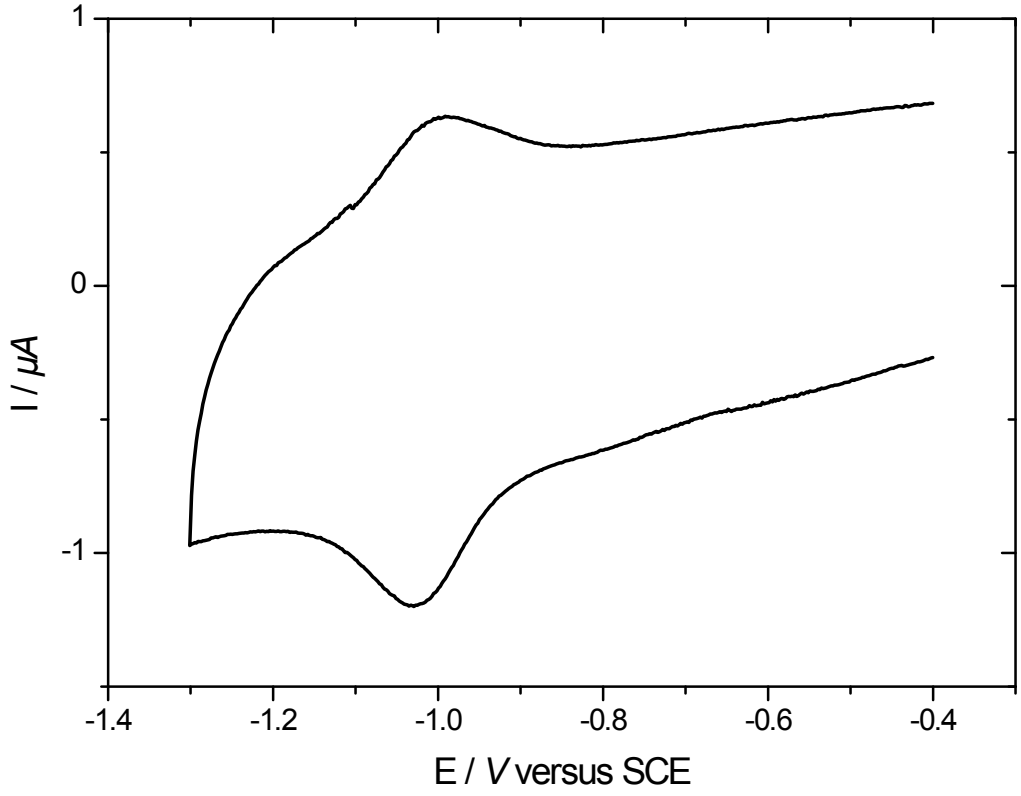

Figure S5. Cyclic voltammogram of a $\mathbf{K^{W}_{Sn}}$-functionalized glassy carbon electrode in a 0.1M $TBAPF_6$ solution in acetonitrile at scan rate of $\nu = 100$ mV.s^{-1}. $E_{1/2}^{red1} = -1.01V_{/SCE}$

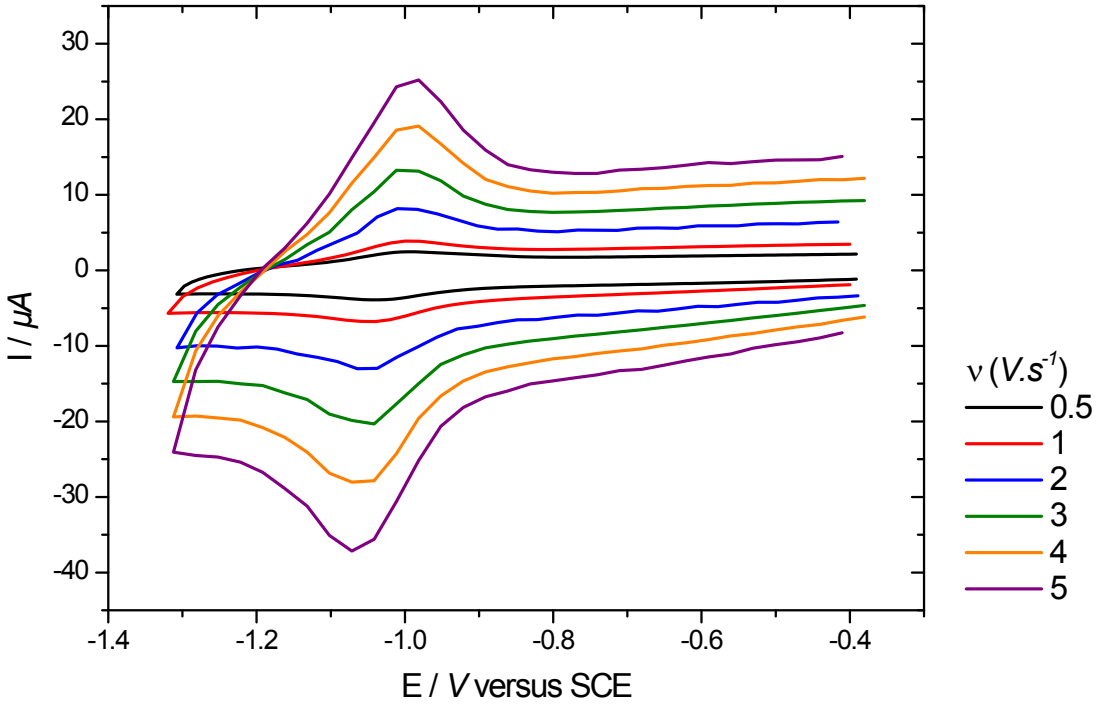

Figure S6. Cyclic voltammograms of a $\mathbf{K^{W}_{Sn}}$-functionalized glassy carbon electrode in a 0.1M $TBAPF_6$ solution in acetonitrile at scan rates of ν = 0.5, 1, 2, 3, 4, 5 $V.s^{-1}$

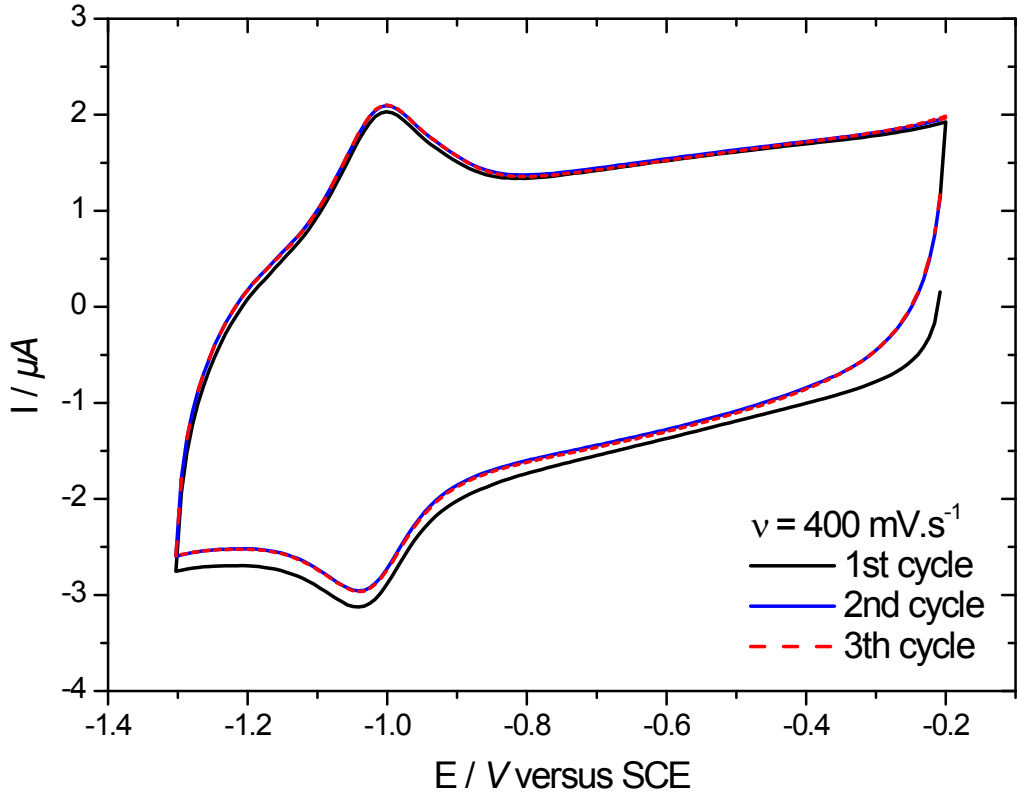

Figure S7. Cyclic voltammograms of a $\mathbf{K^{W}_{Sn}}$-functionalized glassy carbon electrode in a 0.1M $TBAPF_6$ solution in acetonitrile at scan rate of $\nu = 0.4\ V.s^{-1}$

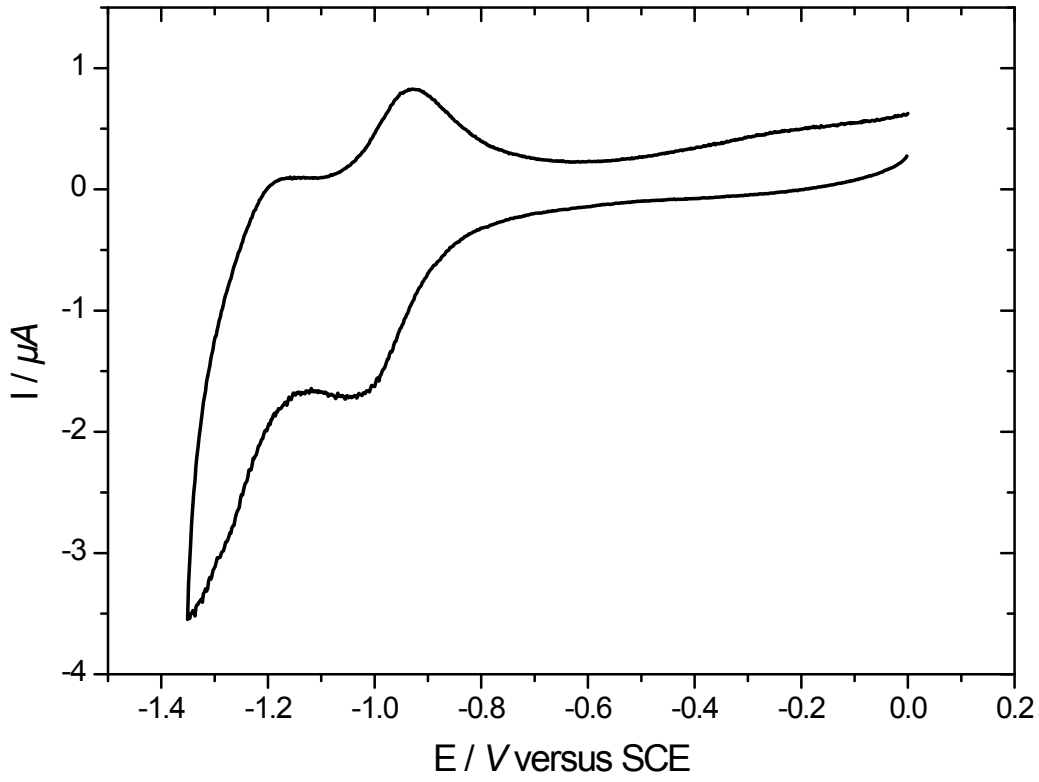

Figure S8. Cyclic voltammogram of a $\mathbf{K^{W}_{Sn}}$-functionalized silicon electrode in a 0.1M $TBAPF_6$ solution in acetonitrile at scan rate of $\nu = 100$ mV.s^{-1}. $E_{1/2}^{red1} = -0.98$ $V_{/SCE}$

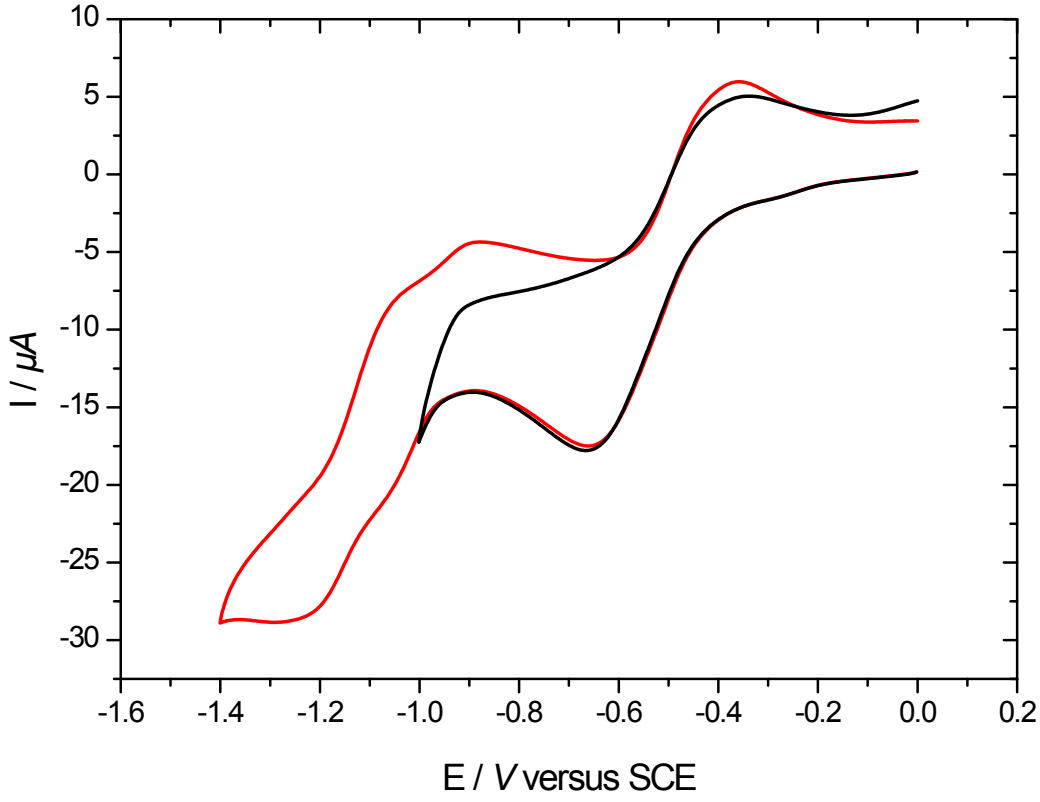

Figure S9. Cyclic voltammogram of $\mathbf{K^{Mo}_{Sn}[N_3Et_2]}$ (1mM) at a GC electrode in a 0.1M $TBAPF_6$ solution in acetonitrile at scan rate of $\nu = 100$ mV.s^{-1}. $E_{1/2}{}^{red1} = -0.50V_{/SCE}$

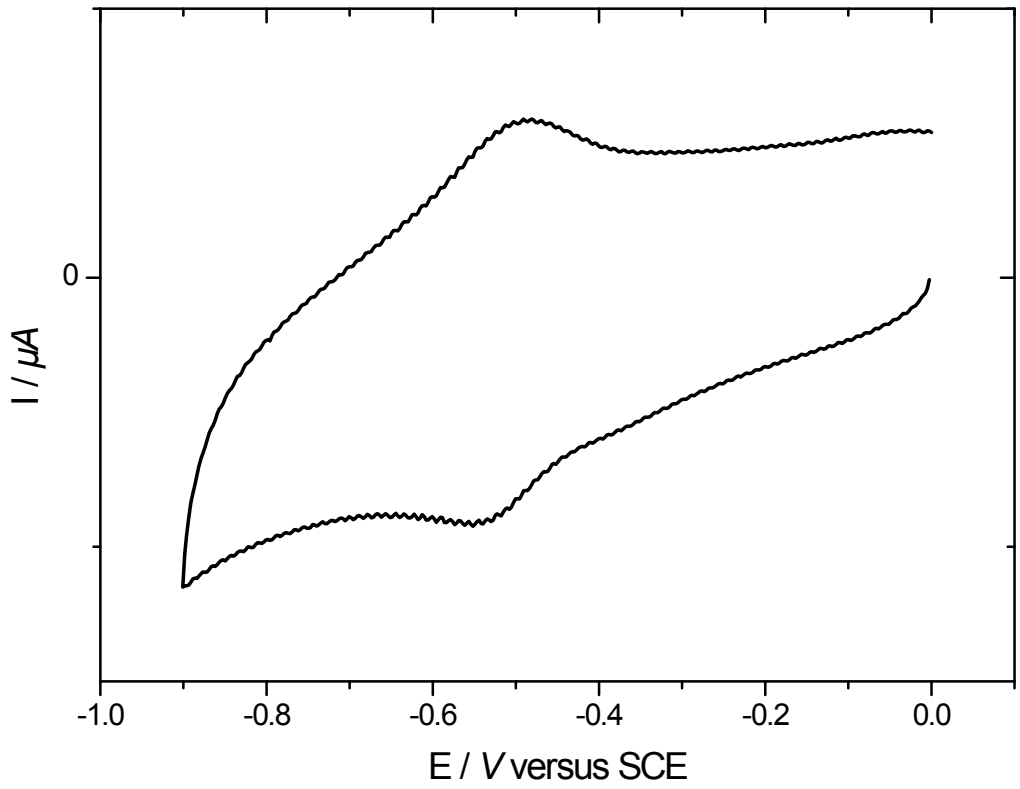

Figure S10. Cyclic voltammogram of a $\mathbf{K^{Mo}_{Sn}}$-functionalized glassy carbon electrode in a 0.1M $TBAPF_6$ solution in acetonitrile at scan rate of $\nu = 100$ mV.s^{-1}. $E_{1/2}{}^{red1} = -0.52V_{/SCE}$

3. XPS characterization

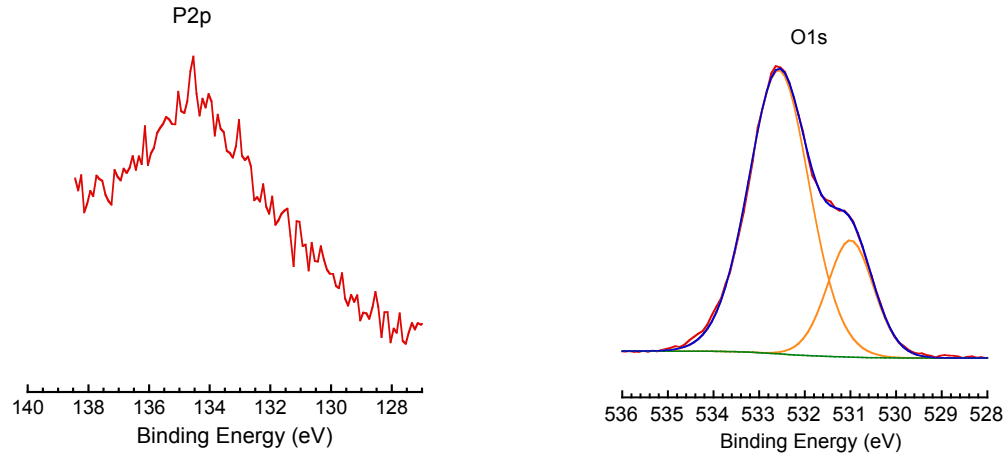

Figure S11. P2p and O1s HR-XPS spectra of $\mathbf{K^{W}_{Sn}}$ modified n-Si(100) substrate. The contribution at 532.6 eV on the O1s photopeak is attributed to oxygen atoms in silicon dioxide. The XPS measurements were performed after numerous characterizations (included solid-state electrical measurements) and oxide may have been formed due to the repeated manipulation of the substrate.

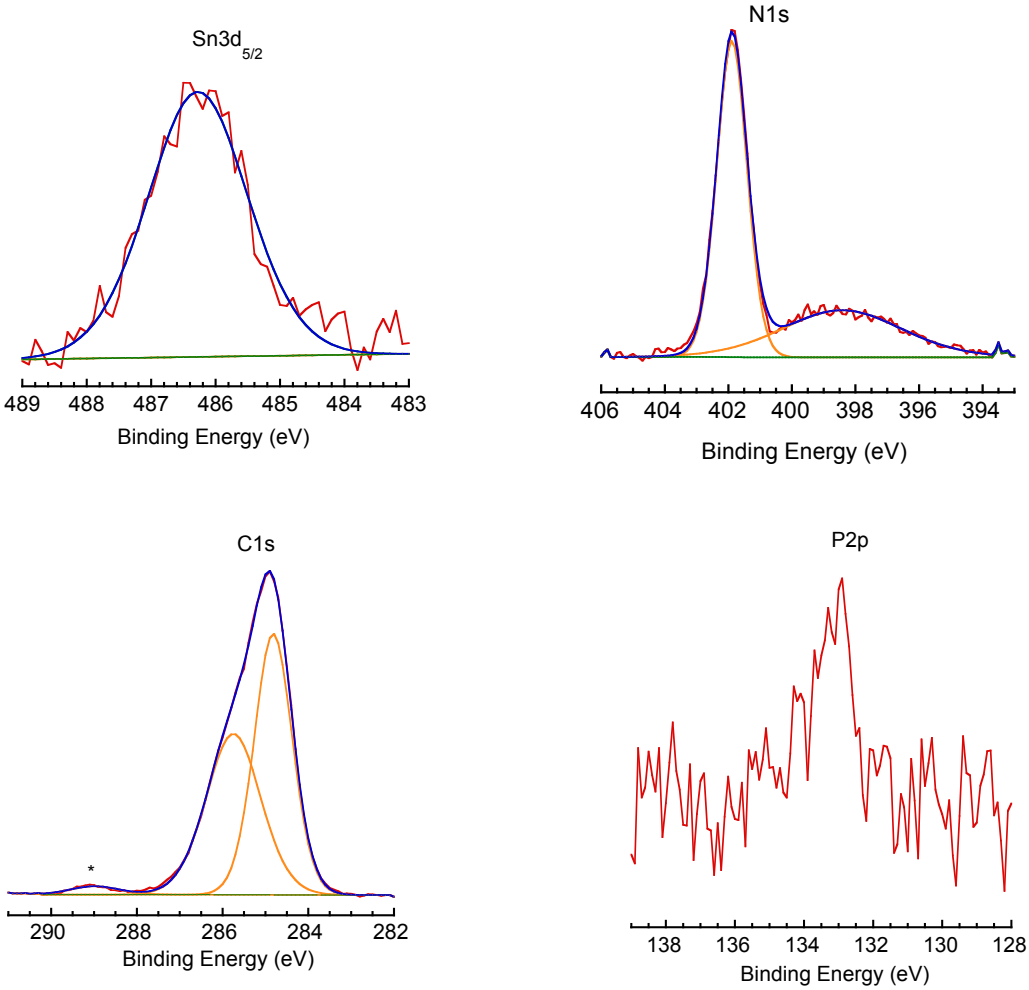

Figure S12. $Sn3d_{5/2}$, N1s, C1s and P2p HR-XPS spectra of a $\mathbf{K^{Mo}_{Sn}[N_2^+]}$ reference powder drop-casted on a Si/SiO_2 substrate. On the N1s spectrum, the broad peak at around 398 eV is attributed to nitrogen derivatives of the unstable diazonium group in the $\mathbf{K^{Mo}_{Sn}[N_2^+]}$ powder.

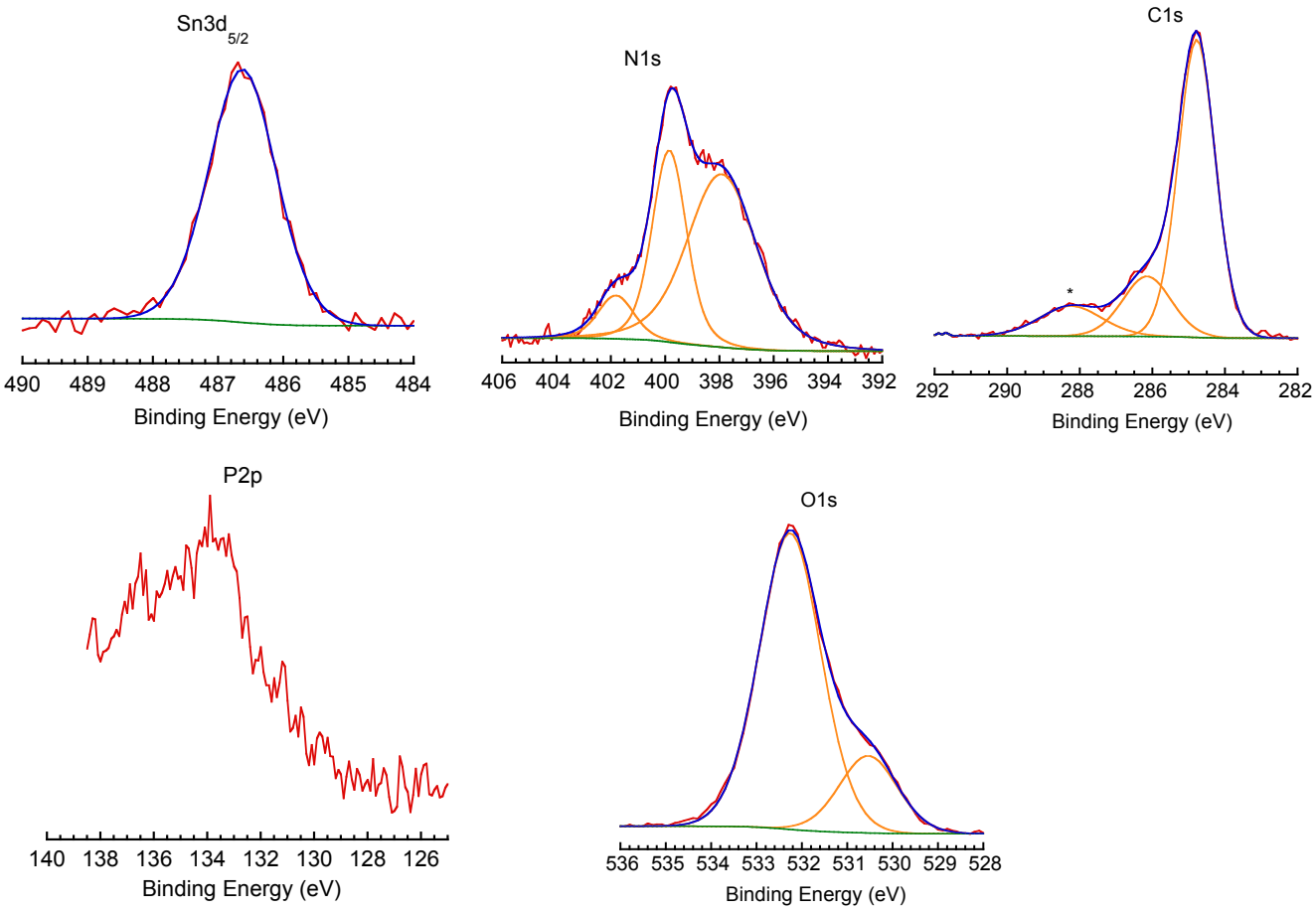

Figure S13. $Sn3d_{5/2}$, N1s, C1s, P2p and O1s HR-XPS spectra of $\mathbf{K^{Mo}_{Sn}}$ modified n-Si(100) substrate. The peak at 397.9 eV on the N1s spectrum corresponds to a satellite of Mo atoms.

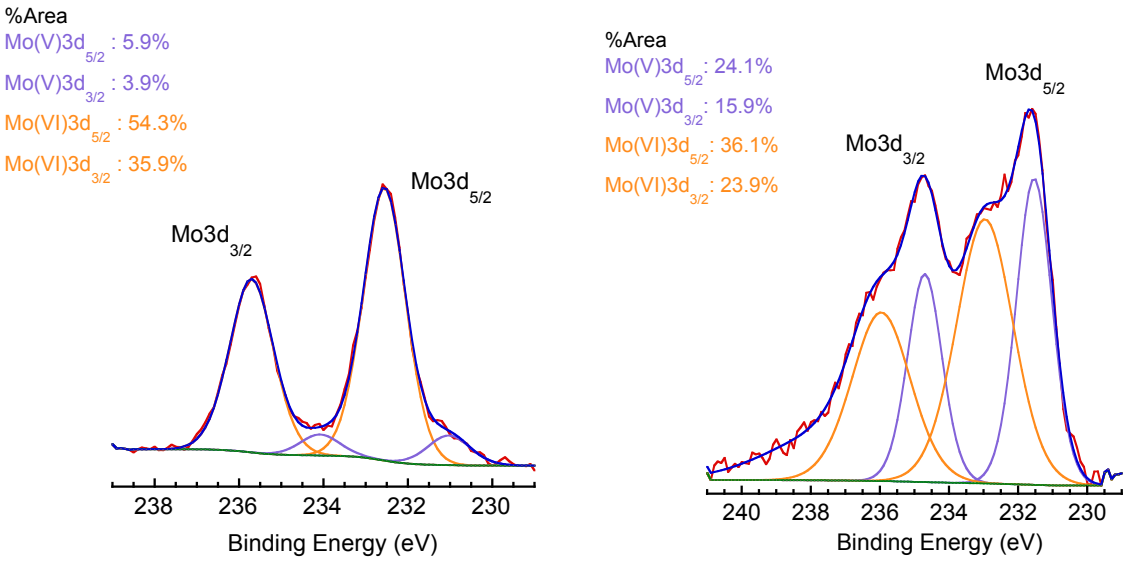

Figure S14. Mo3d HR-XPS spectra of (left) the $\mathbf{K^{Mo}_{Sn}[N_2^+]}$ powder reference and (right) the $\mathbf{K^{Mo}_{Sn}}$ modified n-Si(100) substrate. The same $\mathbf{K^{Mo}_{Sn}[N_2^+]}$ batch was used to measure the powder reference and perform the grafting on hydrogenated silicon.

4. Current histograms at -1V and 1V on K^{W}_{Sn} and K^{Mo}_{Sn} monolayers grafted on highly doped Si substrate

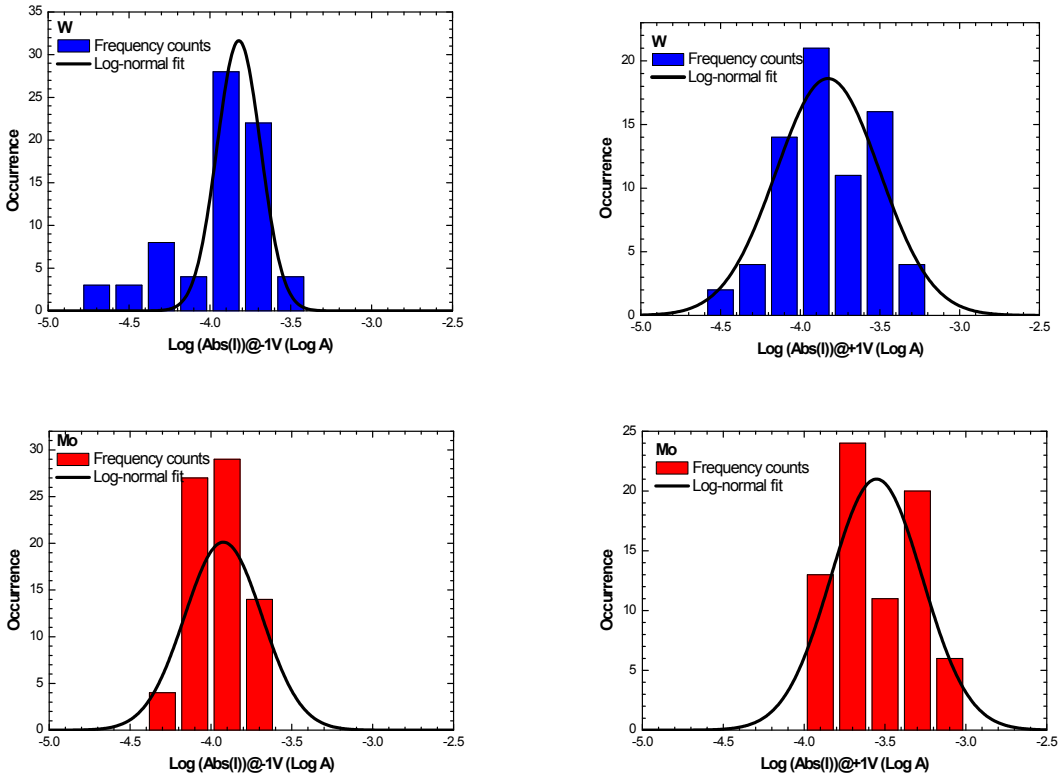

Figure S15. Histograms of the measured current at +1V and -1V for the K^{W}_{Sn} and K^{Mo}_{Sn} samples. They are fitted by one log-normal distribution. In the case of the K^{W}_{Sn} monolayer, the mean values of the current histograms at -1V and +1V are -1.52 x 10^{-4} A and +1.50 x 10^{-4} A, respectively (standard deviations of 0.24 and 0.68). For the K^{Mo}_{Sn} monolayer, the mean values of the current at -1V and +1V are -1.09 x 10^{-4} A and +2.72 x 10^{-4} A (with standard variations of 0.34 and 0.64), leading to a mean rectification ratio I_{+1V}/I_{-1V} of around 2.5.

5. I-V curves adjustment with the Simmon's equation

The expression of the tunnel current through a potential barrier was given by Simmons equation (equation 1):[5]

$$\frac{I}{S}=\frac{e}{4\pi hs^2}\left\{(2\Phi_{POM}-eV)exp-\frac{4\pi s\sqrt{m(2\Phi_{POM}-eV)}}{h}-(2\Phi_{POM}+eV)exp-\frac{4\pi s\sqrt{m(2\Phi_{POM}+eV)}}{h}\right\}$$

(eq. 1)

with e the elementary charge, h Planck's constant, s thickness of the tunneling barrier, Φ barrier height, V voltage applied to the junction, m effective mass of electron, I current and S the electrical contact surface area. The electron effective mass m is separated in $m = m_r . m_0$ with m_0 the mass of electron and m_r the reduced mass.

Adjustments of the measured I-V curves are systematically done for the positive bias (between 0 to 1V, since the I-V curves are quite symmetric with respect of the voltage polarity) by fixing two paramaters (i) s corresponding to the thickness of the monolayer determined by ellipsometry; (ii) and S the surface contact area estimated in our system to ~3 x 10^{-4} cm². This adjustment was realized with Origin 2016 from OriginLab Corp (function "Nonlinear Curve Fit" with the "Levenberg Marquardt" Iteration Algorithm).

6. Histograms of effective mass obtained by Simmon's adjustments on K^{W}_{Sn} and K^{Mo}_{Sn} monolayers

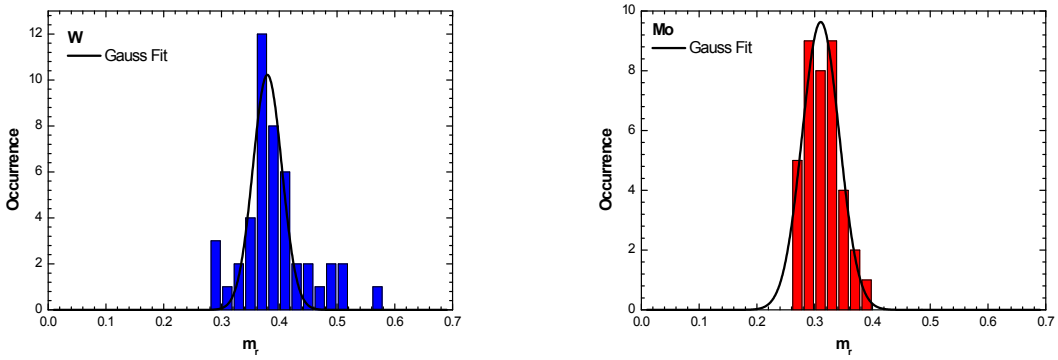

Figure S16. Reduced mass (m_r) histograms obtained by Simmon's adjustments on the different I-V curves, and adjusted by a Gaussian distribution for the K^{Mo}_{Sn} and K^{W}_{Sn} derivatized monolayers. The histograms of m_r are fitted by a Gaussian law. The mean values of m_r for the K^{Mo}_{Sn} and K^{W}_{Sn} monolayers are 0.38 (standard deviation 0.05) and 0.31 (standard deviation 0.06) respectively.

7. AFM image of the neat hydrogenated-Si substrate

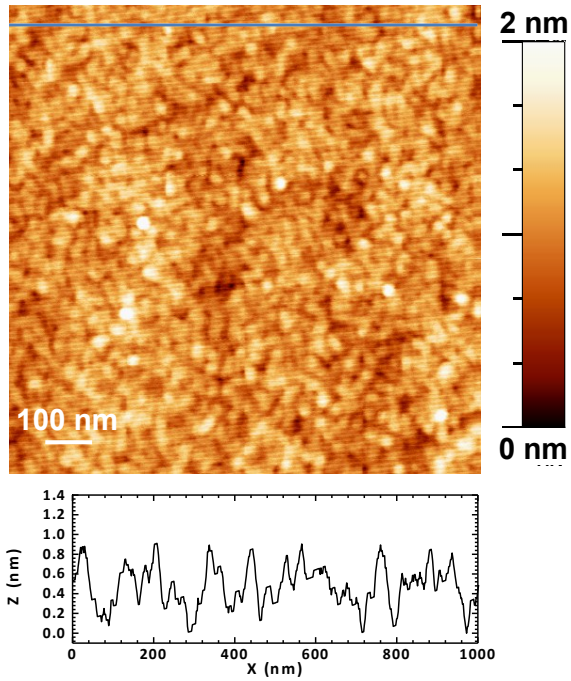

Figure S17. AFM image of the neat hydrogenated-Si substrate (root-mean-squre roughness RMS = 0.25 nm)

References

[1] C. Rinfray, G. Izzet, J. Pinson, S. G. Derouich, J. J. Ganem, C. Combellas, F. Kanoufi, A. Proust, *Chem-Eur J* **2013**, *19*, 13838-13846.

[2] C. Rinfray, V. Brasiliense, G. Izzet, F. Volatron, S. Alves, C. Combellas, F. Kanoufi, A. Proust, *Inorg Chem* **2016**, *55*, 6929-6937.

[3] G. Izzet, F. Volatron, A. Proust, *Chem Rec* **2017**, *17*, 250-266.

[4] C. Rinfray, S. Renaudineau, G. Izzet, A. Proust, *Chem Commun* **2014**, *50*, 8575-8577.

[5] J. G. Simmons, *J Appl Phys* **1963**, *34*, 2581-2590.